Freezing around a finite heat sink immersed in an infinite phase change medium

P. V. Padmanabhan and M. V. Krishnamurthy*

Freezing around a spherical heat sink immersed in an infinite phase change medium – a free boundary problem involving growth and decay of the free boundary – is analysed here. A one-dimensional conduction model is formulated and the resulting partial differential equations are solved by finite difference methods. The energy discharged from the phase change medium during the heat transfer process is analysed for latent heat thermal energy storage applications. Results are presented for a wide range of parameters that are encountered in energy storage devices. The cases of slab/cylindrical heat sink are reexamined for a range of parameters not covered by the earlier investigators

Keywords: *freezing, heat transfer, spherical heat sinks*

When a finite, rigid cold body is suddenly immersed in an infinite pool of a liquid phase change medium (pcm), freezing will be initiated if the temperature of the cold body is less than the freezing point of pcm. When the pcm is initially at its freezing point, freezing continues asymptotically approaching steady-state conditions where the sink surface temperature equals the freezing temperature of the pcm.

If the pcm is initially superheated, there follows a heat transfer process which can be divided into three stages. In the first stage, the temperature of the heat sink increases and freezing continues until a maximum value of crust thickness is reached. In the second stage the frozen pcm starts melting although the sink temperature continues to rise. The second stage comes to an end with the crust totally disappearing when the sink surface temperature equals the freezing temperature of the pcm. In the third stage, which will not be considered in this analysis, single phase heat transfer occurs, raising the temperature of the sink surface to the initial temperature of the pcm. This growth and decay phenomenon is encountered in such processes as dip soldering, dip forming, partial casting and latent heat thermal energy storage (lhtes) devices.

There are two earlier papers[1,2] in this field. Tadjbakhsh and Liniger[1] analysed the case of a slab shaped heat sink in two situations: freezing of water around an ice slab (perturbation); and freezing of solder around a copper rod (perturbation, numerical and experimental).

Their perturbation solutions contain complicated analytical expressions, which are tedious to calculate. Their graphical presentations of results are confined generally to the finite difference solution.

Jiji[2] presented perturbation results for a cylindrical heat sink and some experimental results on the freezing of water around a cold cylinder. That study is restricted to the evaluation and comparison of the crust thickness for a specific experimental run.

The purpose of this paper is to analyse the interface growth, sink temperature and energy transfer for a spherical heat sink. This has applications in direct contact heat exchangers (dche) used in lhtes devices in which a heat transfer fluid (lower in density and immiscible with the pcm) is introduced at the bottom of the storage vessel (containing pcm) as a dispersed phase. Bubbles of this fluid rising through the vessel transfer heat to or from the pcm. Typical examples of the heat transfer fluid and the pcm are Varasol (oil) and Glauber's salt respectively. The previous investigations reported on this problem concerned themselves with the selection and testing of a suitable heat transfer oil for various salt hydrates[3-5], hydrodynamic design procedures[6,7] and conceptual design to overcome the problem of oil nozzle blockage[8] etc, but the phase change heat transfer aspects in dche have not been investigated at all.

In this analysis, the heat transfer fluid drop is idealised to be spherical and assumed to be stationary to provide a rough estimate of the quantity of energy transfer and the maximum drop residence time. However, to have a generalised governing equation for all geometries, a shape factor S is introduced[9], where:

$S=0$ for a slab insulated on one side
$S=0.5$ for a flat cylinder transferring heat on one side, with small ratio of depth to diameter
$S=1$ for an infinitely long cylinder
$S=1.5$ for a football-shaped (ellipsoid) object
$S=2$ for a sphere

To model the growth and decay phenomenon, the following simplifying assumptions are used:

(a) thermophysical properties of the heat sink are independent of temperature;
(b) the freezing temperature T_f^* is single valued;
(c) thermophysical properties of the pcm, although different for the two phases, are constant within a phase;
(d) heat transfer in the pcm is by one dimensional conduction only. Shifting of the freeze front due to density difference in the two phases is neglected;

* Refrigeration and Airconditioning Laboratory, Department of Mechanical Engineering, Indian Institute of Technology, Madras 600036, India
Received 4 June 1984 and accepted for publication on 11 February 1985

(e) the heat sink is assumed to be thermally lumped. This assumption will allow extension of this analysis to the case of a translating heat sink.

Formulation of the problem

Physical model

The physical model and the coordinate system are shown in Fig 1. A rigid heat sink of simple geometry, initially at a uniform temperature $T^*_{d,in}$ is suddenly immersed in an infinite quantity of liquid pcm initially at a uniform temperature T^*_{in} which is greater than its freezing temperature T^*_f. For $T^*_{in} > T^*_f > T^*_{d,in}$ freezing will occur first, followed by melting.

Mathematical model

Application of the conservation laws together with the assumptions mentioned earlier, yields the following set of equations:

Solid phase:

$$(\partial^2 T^*_s/\partial r^{*2}) + (S/r^*)(\partial T^*_s/\partial r^*) = (\partial T^*_s/\partial t)/a_s \qquad (1a)$$

in $r^*_f \geq r^* \geq r^*_d$

Liquid phase:

$$(\partial^2 T^*_l/\partial r^{*2}) + (S/r^*)(\partial T^*_l/\partial r^*) = (\partial T^*_l/\partial t)/a_l \qquad (1b)$$

in $r^* \geq r^*_f$

At the interface between the frozen pcm and the heat sink:

$$T^*_s = T^*_d \quad \text{at} \quad r^* = r^*_d \qquad (1c)$$

$$\lambda_s(\partial T^*_s/\partial r^*) = (\rho c r^*)_d(\mathrm{d}T^*_d/\mathrm{d}t)/(S+1) \qquad (1d)$$

at $r^* = r^*_d$

At the freezing front:

$$T^*_l = T^*_s = T^*_f \quad \text{at} \quad r^* = r^*_f \qquad (1e)$$

$$\lambda_s(\partial T^*_s/\partial r^*) - \lambda_l(\partial T^*_l/\partial r^*) = \rho_s \Delta h(\mathrm{d}r^*_f/\mathrm{d}t) \qquad (1f)$$

at $r^* = r^*_f$

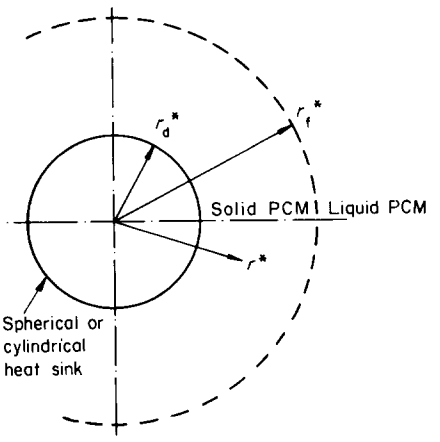

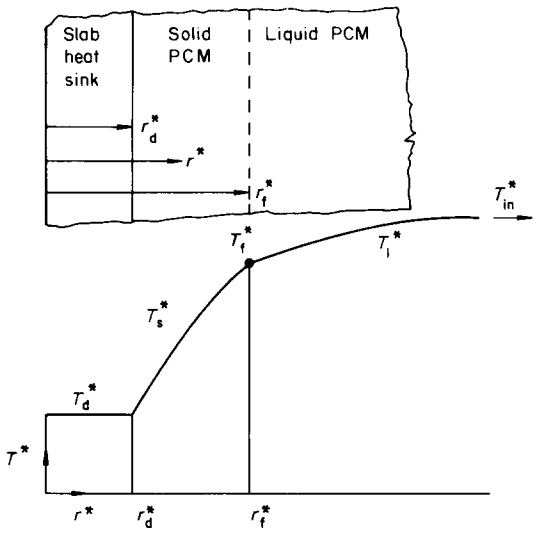

Fig 1 Physical model and coordinate system

Notation

a	Thermal diffusivity
c	Specific heat
E^*_{max}	Maximum possible energy transfer, Eq (21)
E_1, E_2, E_3, E_4, E_5	Normalised components of energy transfer, Eqs (22)–(26)
Fo	Fourier number, $a_s t/r^{*2}_d$
Fo^+	Time at which the decay of the free boundary starts
Fo^{++}	Crust life time
ΔFo	Time step size
Δh	Latent heat of fusion of the phase change medium (pcm)
n	Number of equal divisions in the frozen pcm
p	Root of Neumann's transcendental equation, Eq (17)
r^*	Space coordinate
r	Normalised space coordinate, $(r^* - r^*_d)/r^*_d$
r^+_f	Freeze front thickness at Fo^+
S	Sink shape factor (0—slab; 1—cylinder; 2—sphere)
Ste	Stefan number, $c_s(T^*_{in} - T^*_{d,in})/\Delta h$
t	Time
T^*	Temperature
T	Normalised temperature, $(T^* - T^*_{d,in})/(T^*_{in} - T^*_{d,in})$
V^*	Volume of heat sink
w	Heat capacity ratio, $(\rho c)_d/(\rho c)_s$
η	Transformed space coordinate, r/r_f
η_{max}	point at which $\left\|\frac{\partial T}{\partial \eta}\right\| = 0.001$
$\Delta\eta$	Space step size
λ	Thermal conductivity
ρ	Density
ϕ	r^2_f

Subscripts

d	Heat sink
d,in	Initial condition of heat sink
f	Condition at the moving boundary
i	Space step index
in	Initial condition of pcm
j	Time step index
l	Liquid pcm
s	Solid pcm

As $r^* \to \infty$, $T_l^* \to T_{in}^*$ (1g)

Initial conditions are:

$T_s^* = T_{s,in}^*$ at $t=0$ (1h)

$T_l^* = T_{in}^*$ at $t=0$ (1i)

$r_f^* = r_d^*$ at $t=0$ (1j)

The following dimensionless variables are introduced to normalise the equations:

$$T = (T^* - T_{s,in}^*)/(T_{in}^* - T_{s,in}^*) \quad (2)$$

$$r = (r^* - r_d^*)/r_d^* \quad (3)$$

$$Fo = a_s t/r_d^{*2} \quad (4)$$

$$w = (\rho c)_d/(\rho c)_s \quad (5)$$

$$Ste = c_s(T_{in}^* - T_{s,in}^*)/\Delta h \quad (6)$$

The numerical, finite difference solution of these equations needs complex programming in view of the time-varying space domain. Of the methods available to overcome this difficulty, the enthalpy method[10] is simple to program and gives fairly accurate results for the temperature profile. But, as observed by Bell[11], time–temperature histories obtained with this method contain a number of false plateaus and are far from acceptable. Therefore, the enthalpy method needs further modifications[11].

The boundary fixing technique using Landau[12] type transformation is used here. The moving boundary is immobilised by the use of the following transformations:

$$\eta = r/r_f \quad (7)$$

$$\phi = r_f^2 \quad (8)$$

Boundary immobilisation has the advantage of giving a time-invariant space domain, but the energy equations become more involved. The transformed equations are:

$$\frac{\partial^2 T_s}{\partial \eta^2} + \frac{\partial T_s}{\partial \eta}\left\{\frac{S\phi^{1/2}}{(1+\eta\phi^{1/2})} + \frac{\eta}{2}\frac{d\phi}{dFo}\right\} = \frac{\phi \partial T_s}{\partial Fo} \quad (9a)$$

in $1 \geq \eta \geq 0$

$$\frac{\partial^2 T_l}{\partial \eta^2} + \frac{\partial T_l}{\partial \eta}\left\{\frac{S\phi^{1/2}}{(1+\eta\phi^{1/2})} + \frac{a_s \eta}{a_l}\frac{d\phi}{2dFo}\right\} = \frac{a_s}{a_l}\frac{\phi \partial T_l}{\partial Fo} \quad (9b)$$

in $\eta \geq 1$

$T_s = T_d$ at $\eta = 0$ (9c)

$(\partial T_s/\partial \eta) = w\phi^{1/2}(dT_d/dFo)/(S+1)$ at $\eta = 0$ (9d)

$T_l = T_s = T_f$ at $\eta = 1$ (9e)

$(\partial T_s/\partial \eta) - (\lambda_l/\lambda_s)(\partial T_l/\partial \eta) = (d\phi/dFo)/(2Ste)$ at $\eta = 1$ (9f)

$T_l \to 1$ as $\eta \to \infty$ (9g)

$T_d = 0$ at $Fo = 0$ (9h)

$T_l = 1$ at $Fo = 0$ (9i)

$\phi = 0$ at $Fo = 0$ (9j)

Numerical scheme

A finite difference method is adopted for solving Eq (9). The frozen region ($1 \geq \eta \geq 0$) is subdivided into n equal divisions with a space increment of $\Delta\eta$. Subscripts $i=1$ and $i=n+1$ denote the boundary $\eta=0$ and $\eta=1$ respectively. Time is indexed by subscript j, with $Fo=0$ at $j=0$.

Using suitable analogues, the following difference equations can be obtained:

$$\phi_{j+1} = \phi_j + [Ste\Delta Fo/(3\Delta\eta)][(11T_f - 18T_{n,j} + 9T_{n-1,j} - 2T_{n-2,j}) - (\lambda_l/\lambda_s)(-11T_f + 18T_{n+2,j} - 9T_{n+3,j} + 2T_{n+4,j})] \quad (10)$$

$$T_{d_{j+1}} = T_{d_j}[1 - 11(S+1)\Delta Fo/(6w\Delta\eta\phi_j^{1/2})] + [(S+1)\Delta Fo/(6w\Delta\eta\phi_j^{1/2})](18T_{2,j} - 9T_{3,j} + 2T_{4,j}) \quad (11)$$

$$T_{i-1,j+1}(PP - QQ_i) - T_{i,j+1}(2PP + RR) + T_{i+1,j+1}(PP + QQ_i) = -RRT_{i,j} \quad (12)$$

where:

$$PP = 1/(\Delta\eta)^2 \quad (13)$$

$$RR = \begin{cases} \phi_{j+1}/\Delta Fo & \text{in } 2 \leq i \leq n \\ (a_s/a_l)\phi_{j+1}/\Delta Fo & \text{in } i \geq (n+2) \end{cases} \quad (14)$$

$$QQ_i = \begin{cases} \left[\frac{S\phi_{j+1}^{1/2}}{(1+\eta_i\phi_{j+1}^{1/2})} + \frac{\eta_i(\phi_{j+1} - \phi_j)}{2\Delta Fo}\right] \Big/ (2\Delta\eta) & \text{in } 2 \leq i \leq n \\ \left[\frac{S\phi_{j+1}^{1/2}}{(1+\eta_i\phi_{j+1}^{1/2})} + \frac{a_s\eta_i(\phi_{j+1} - \phi_j)}{a_l 2\Delta Fo}\right] \Big/ (2\Delta\eta) & \text{in } i \geq (n+2) \end{cases} \quad (15)$$

Eqs (10) and (11) explicitly give the thickness of freeze front and the sink temperature respectively. Eq (12) is implicit and leads to a tridiagonal matrix which is solved by Thomas' algorithm[13] to get the temperature profiles in the pcm.

Computational procedure

Since the frozen region of pcm is non-existent at zero time, some of the terms in Eqs (10)–(12) are either indeterminate or infinite[14]. Therefore a starting solution, which gives all the values at time step $j=1$, is a pre-requisite to this scheme. By the same argument, the solution must be stopped just before the freeze front thickness becomes zero.

To start the solution, it is assumed that Neumann's exact, closed form analytical solution for a semi-infinite planar pcm with an isothermal wall, is valid for the present problem also at time step $j=1$. Then:

$$r_f = \phi^{1/2} = 2pFo^{1/2} \quad (16)$$

where p is the root of the transcendental equation:

$$T_f - \frac{\lambda_l}{\lambda_s}\left(\frac{a_s}{a_l}\right)^{1/2}(1 - T_f)\frac{\operatorname{erf}(p)\exp(p^2(1 - a_s/a_l))}{\operatorname{erfc}(p(a_s/a_l)^{1/2})} = \frac{p\pi^{1/2}\operatorname{erf}(p)\exp(p^2)}{Ste} \quad (17)$$

Neglecting the heat capacity of the frozen pcm, the sink temperature may be approximated as:

$$T_d = (S+1)\phi^{1/2}/(wSte) \quad (18)$$

The temperature profiles in the pcm can then be written as:

$$T_i = T_d + (T_f - T_d)\frac{\operatorname{erf}(p\eta_i)}{\operatorname{erf}(p)} \quad \text{in} \quad 2 \leq i \leq n$$

$$T_i = 1-(1-T_f)\frac{\operatorname{erfc}(p\eta_i(a_s/a_l)^{1/2})}{\operatorname{erfc}(p(a_s/a_l)^{1/2})} \quad \text{in} \quad i \geqslant (n+2) \qquad (19)$$

Now that the values are known at time step $j=1$, Eqs (10)–(12) can be solved repeatedly in the same order, to get the values for time steps $j \geqslant 2$.

The solution is stopped when the sink temperature reaches 0.9999 T_f and the curve r_f versus Fo is linearly extrapolated as suggested by Murray and Landis[14]. The extrapolation gives the crust life time Fo^{++}. Solution of these equations is obtained on an IBM 370/155 digital computer.

Since the rate of growth of the freeze front is faster than its decay (as will be seen later), from the stand point of accuracy and cpu time, an initial time step of $\Delta Fo = 1 \times 10^{-6}$ is used while starting the solution. The time step size is doubled at the end of every 10 time steps. A space step size of $\Delta\eta = 0.1$ ($n=10$) was uniformly used, throughout the calculations.

The liquid pcm region extends from $\eta = 1$ to $\eta = \infty$. The latter value cannot be accommodated in the computer so the solution domain is restricted to $\eta = \eta_{max}$, when η_{max} is taken as the smallest value of η at which the gradient $(\partial T/\partial\eta) \leqslant 0.001$. At each time step, the value of η_{max} will be changing and is fixed iteratively in the program by checking the gradients.

During the later stages, particularly during the decay of the freeze front, the value of η_{max} is excessively large and the cpu time for each time step becomes prohibitively costly. This is an added reason for stopping the solution at $T_d \geqslant 0.9999\ T_f$.

Steady state conditions and energy components

Steady state will be reached when the sink surface temperature equals the initial temperature T^*_{in} of the pcm. If the liquid pcm is initially not at its freezing point, then the steady state will be reached at the end of the third stage of the heat transfer process. The freeze front would have disappeared at the beginning of the third stage itself. Hence the steady state crust thickness is zero whenever the liquid pcm is initially superheated.

If the liquid pcm is initially saturated, only the frozen region need be analysed and an energy balance can be written for the steady-state conditions, when the heat sink and pcm are at T_f^*. At steady state conditions, the following relation can be derived:

$$r_f = [(1+wSte)^{1/(S+1)} - 1] \qquad (20)$$

Obviously the freeze front thickness at any other time and any other initial conditions, will be lower than that given by Eq (20).

Since thermal energy storage is the motivation for this investigation, it will be interesting to identify and study the various energy components associated with this phase change problem. There are two such components for freezing initiated without liquid superheat and four components when there is liquid superheat. Here again, the components are normalised by E^*_{max}, the maximum possible energy that could be extracted by the heat sink, ie:

$$E^*_{max} = (V^*\rho t)_d(T^*_{in} - T^*_{d,in}) \qquad (21)$$

The total energy extracted by the heat sink and the four components of energy released by the pcm are given below after normalisation:

$$E_1 = T_i \qquad (22)$$

$$E_2 = \frac{(1+r_f)^{S+1}-1}{wSte} \qquad (23)$$

$$E_3 = \frac{[(1+r_f)^{S+1}-1](1-T_f)(a_s/a_l)(\lambda_l/\lambda_s)}{w} \qquad (24)$$

$$E_4 = \frac{(S+1)r_f}{w}\int_0^1 (1+\eta r_f)^S(T_f - T_s)\,d\eta \qquad (25)$$

$$E_5 = E_1 - (E_2+E_3+E_4) \qquad (26)$$

E_2 is the latent heat released by the freezing process. The component E_3 is the sensible energy released by the liquid pcm in the region $r_d^* \leqslant r^* \leqslant r_f^*$ while it is cooled from T^*_{in} to T_f^*. This component becomes zero for initially saturated liquid pcm. E_4 is the energy that is released as sensible heat by the subcooling of the frozen solid below the phase change temperature. Evaluation of E_4 is by numerical integration of the temperature profile using Simpson's 1/3rd rule. The last energy component E_5 is the sensible energy released from the unfrozen liquid pcm in the region $r^* \geqslant r_f^*$. E_5 is zero for saturated liquid pcm.

Comparison with earlier work

Numerical results of Tadjbakhsh and Liniger[1] for the crust thickness in dip soldering are compared with the results from the present model in Fig 2. For the sake of completeness, the series solution given by them is applied and evaluated for this problem. The parameters used in this comparison are $Ste = 0.1522456$, $w = 2.206885$, $T_f = 0.32815$, $\lambda_s/\lambda_l = 2.037735$ and $a_l/a_s = 0.491166$.

Their results predict a larger crust thickness than that predicted by the present model. Though experiments have been performed by them, the crust thickness values were not presented. Further, details of their numerical scheme, such as step sizes, iteration scheme, etc. are not given in their paper. Thus it is difficult to comment on the accuracy of the results.

In spite of the fact that our model treats the heat sink as a lumped system and not as a distributed system,

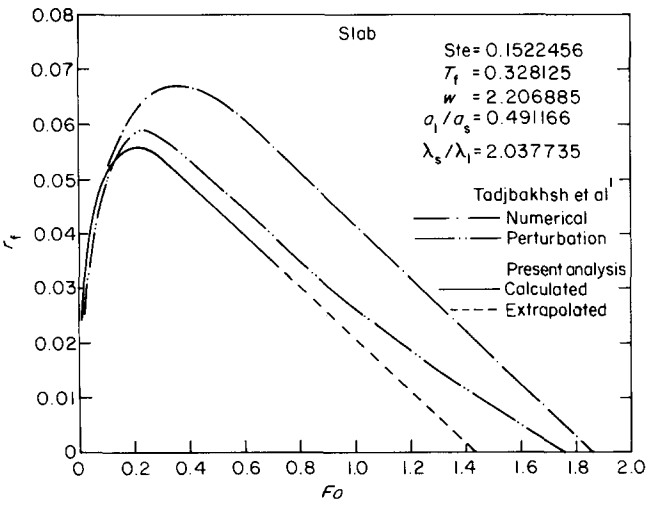

Fig 2 Freezing of solder around a copper rod

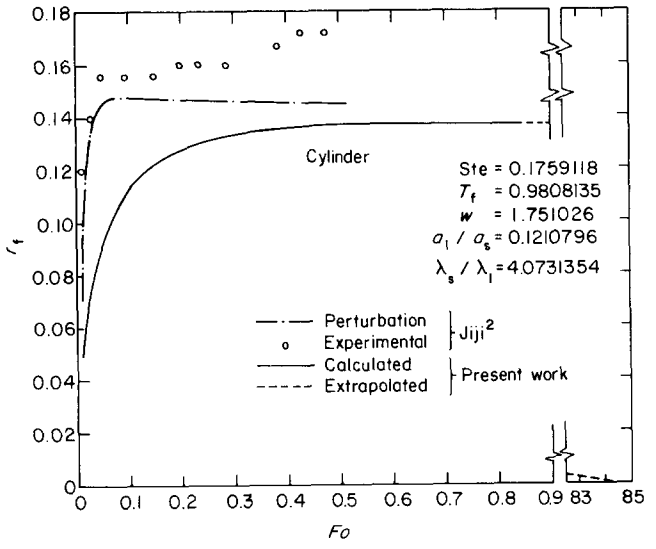

Fig 3 Freezing of water over a steel cylinder

Table 1 Thermophysical properties of steel and water

Property	Material		
	Steel	Water	Ice
Density, kg/m^3	7835	1002	920
Specific heat, kJ/(kg K)	0.465	4.216	2.261
Thermal conductivity, W/(m K)	—	0.5524	2.25
Thermal diffusivity, m^2/h	0.053	471×10^{-6}	3890×10^{-6}
Latent heat, kJ/kg	—		334.95
Fusion temperature, K	—		273

their perturbation results are closer to the present numerical results than their numerical results.

The results of Jiji[2] for the freezing of water around a steel cylinder are compared with our model in Fig 3. The parameters are $Ste=0.1759118$, $w=1.7510264$, $T_f=0.9808135$, $\lambda_s/\lambda_l=4.0731354$, $a_l/a_s=0.1210796$. Thermophysical properties of steel and water used in the analysis are listed in Table 1.

Discrepancies between the results of the two investigations could not be analysed as Jiji[2] has not specified the values of the thermophysical properties he used.

Results and discussion

Results were obtained for the following heat sink geometries:

slab insulated at one end
cylinder
sphere

The range of values used in the parametric analysis was:

Ste = 0.1–1.3
w = 0.6–1.4
T_f = 0.7–1.0
λ_s/λ_l = 0.5–1.5
a_l/a_s = 0.5–1.5

The values are typical of direct contact lhtes devices (Table 2).

Time histories of crust thickness and sink temperature

The effects of Stefan number on the time history of crust thickness and sink temperature are shown in Fig 4. The freeze front progress is retarded at smaller Stefan numbers. With increasing Stefan numbers the maximum crust thickness r_f^+ increases. The duration Fo^{++} of two-phase heat transfer appears to be insensitive to Stefan number at higher values of Ste. The sink temperature is higher for lower Stefan numbers at all times.

The effect of the heat capacity ratio w on the crust thickness and sink temperature is shown in Fig 5. This is an important parameter that significantly affects the crust thickness. Both the maximum crust thickness r_f^+ and the process time Fo^{++} are considerably higher for larger values of w. The sink temperature, however, exhibits the opposite effect. The larger the value of w the smaller is the sink temperature at small times and it has negligible effect on the sink temperature at large times. The superheat parameter T_f is a more significant parameter (Fig 6). For a

Table 2 Properties of pcm and immiscible oils[+]

Property		pcm	
		$NaNO_3$–KNO_3[++] eutectic	Glauber's Salt ($Na_2SO_4.10H_2O$)
Fusion temperature, K		495	305
Heat of fusion, J/kg		137.3×10^3	251×10^3
Thermal conductivity, W/(K m)	Solid	0.484516	0.514
	Liquid	0.571131	0.589
Specific heat, J/(K kg)	Solid	1507.25	1920
	Liquid	1507.25	3260
Density, kg/m^3	Solid	2180	1460
	Liquid	1880	1330

	Immiscible oil	
	Hytherm-500 for high temperature	Varasol for low temperature
Density, kg/m^3	708	800
Specific heat, J/(K kg)	2964	2093

[+] Properties taken from Refs 6, 15–18
[++] 46% $NaNO_3$–54% KNO_3 by weight; referred to as eutectic for convenience.

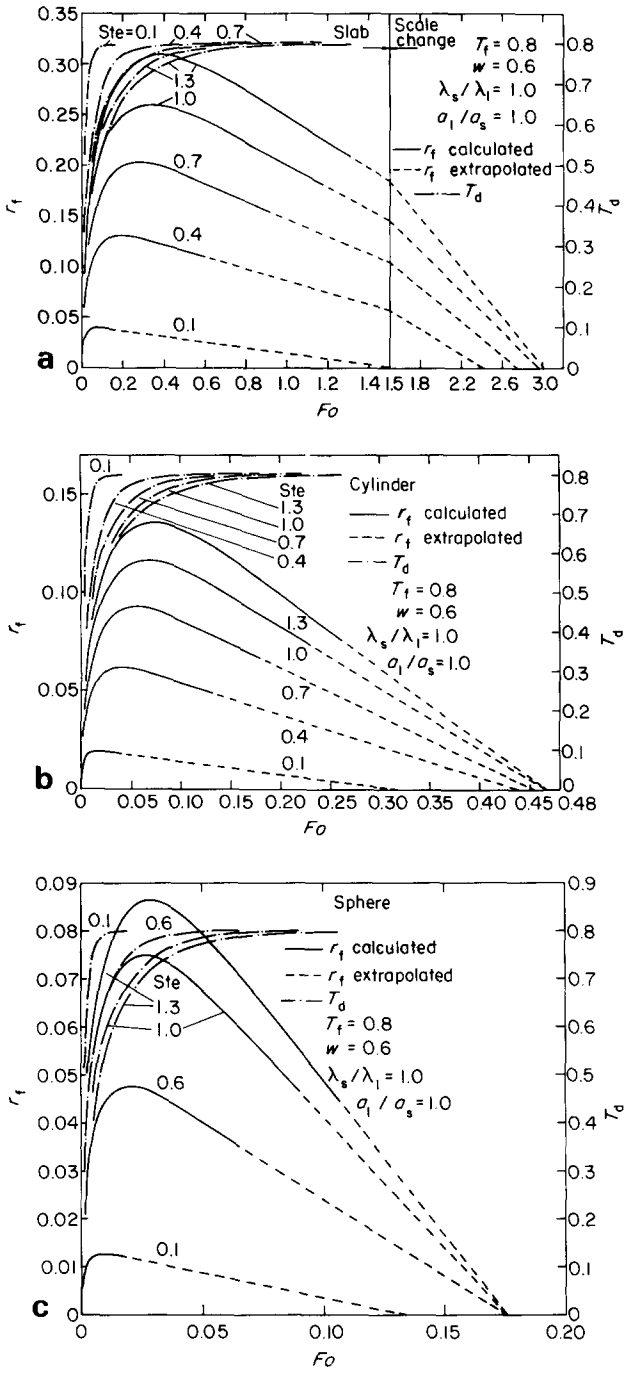

Fig 4 Effect of Ste *on* r_f *and* T_d *(a) slab insulated at one end (b) cylinder (c) sphere*

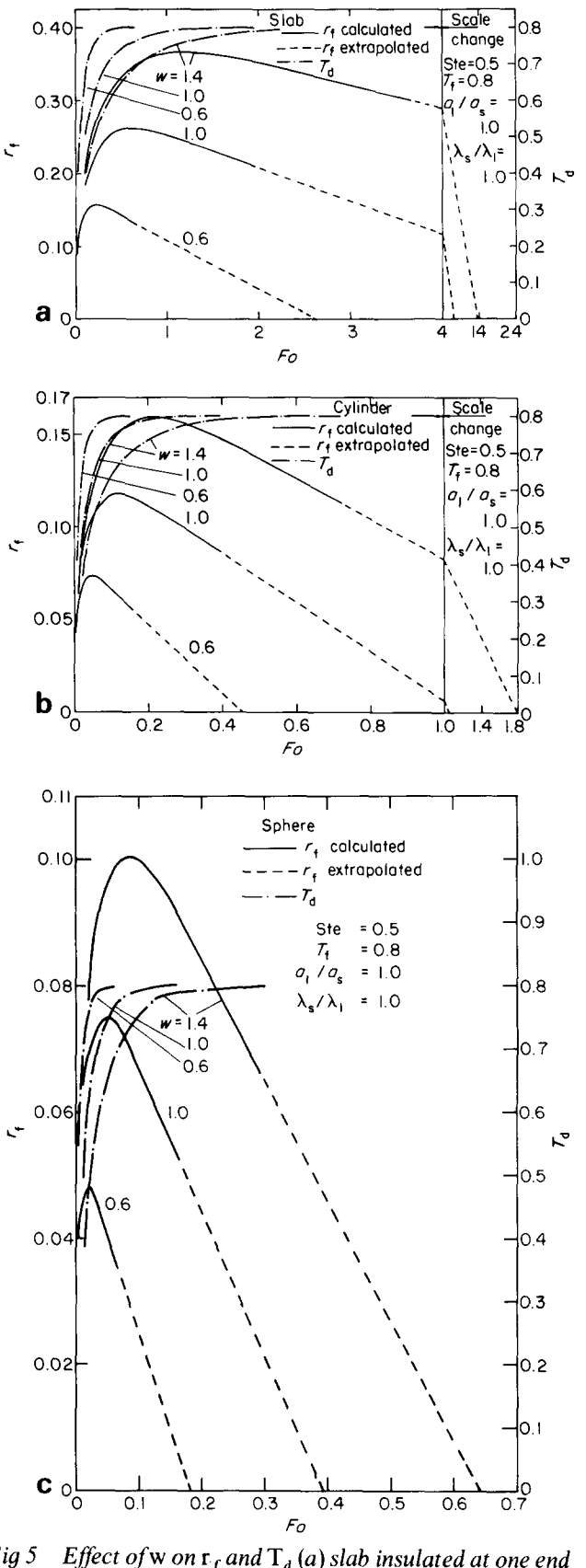

Fig 5 Effect of w *on* r_f *and* T_d *(a) slab insulated at one end (b) cylinder (c) sphere*

pcm initially at its saturation temperature, T_f is unity. Smaller values of T_f indicate greater superheat of pcm. Both the crust thickness and the sink temperatures are considerably higher for larger T_f values. The values of r_f^+, Fo^+ and Fo^{++} are significantly greater for smaller superheat of pcm. It is to be noted that for $T_f = 1$, there is no decay and the crust thickness increases asymptotically towards a steady-state value. The steady-state crust thickness obtained numerically agrees closely with that given by Eq (20) for all the three geometries investigated.

The change in the thermal conductivity due to phase change, expressed by λ_s/λ_l affects the heat transfer process as shown in Fig 7. Increase in the pcm solid to liquid conductivity ratio accelerates the freeze front movement and decelerates the decay of the freeze front. Correspondingly the sink temperature changes more slowly for larger values of λ_s/λ_l.

The pcm liquid to solid diffusivity ratio also influences the two-phase heat transfer as shown in Fig 8.

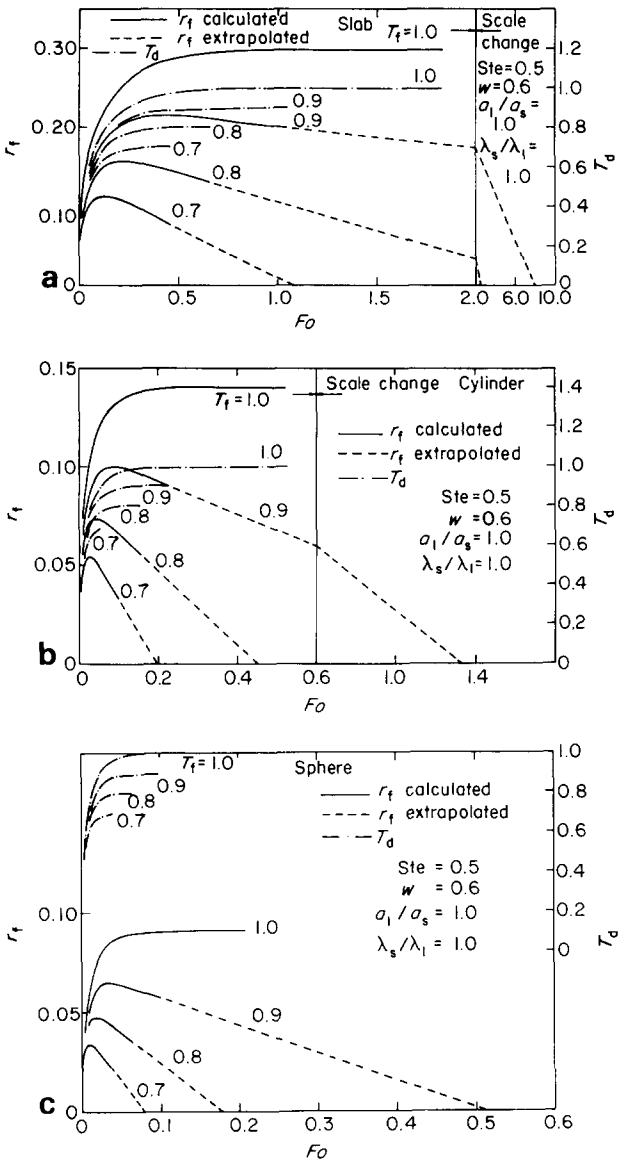

Fig 6 Effect of T_f *on* r_f *and* T_d *(a) slab insulated at one end (b) cylinder (c) sphere*

Here also it is seen that higher values of a_l/a_s produce larger crust thickness and lower sink temperatures.

Energy storage

Various energy components defined in Eqs (22)–(26) are estimated for the various parameters. Since the oil drop in the immiscible oil-direct contact lhtes is idealised to be a sphere, the analysis was restricted to the spherical heat sink.

Figs 9–11 show the time variation of E_1, E_2, E_2+E_4 and $E_2+E_4+E_3$. Wherever the curve E_2+E_4 is not shown, it is to be taken that E_4 is so small that it could not be plotted separately.

It is seen that for a given set of parameters, all the components except E_5 follow a pattern similar to that of the freeze front. That is, during the growth of the freeze front they increase, and during the decay of the phase change boundary they decrease.

The sensible heat of the unfrozen region, E_5 increases both during the growth and decay of the fusion

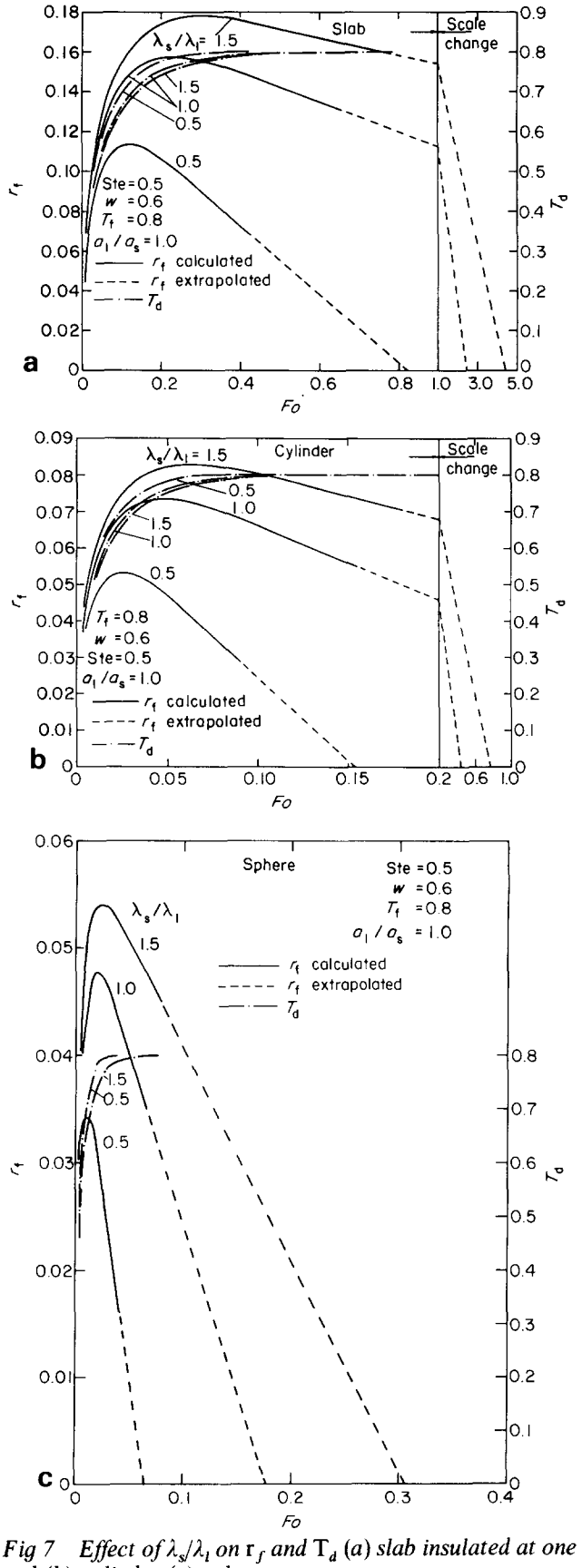

Fig 7 Effect of λ_s/λ_l *on* r_f *and* T_d *(a) slab insulated at one end (b) cylinder (c) sphere*

front. The increase is faster during the decay period. The reason is that as the freeze front grows, only the heat transfer fluid drop acts as the sink, while during its decay,

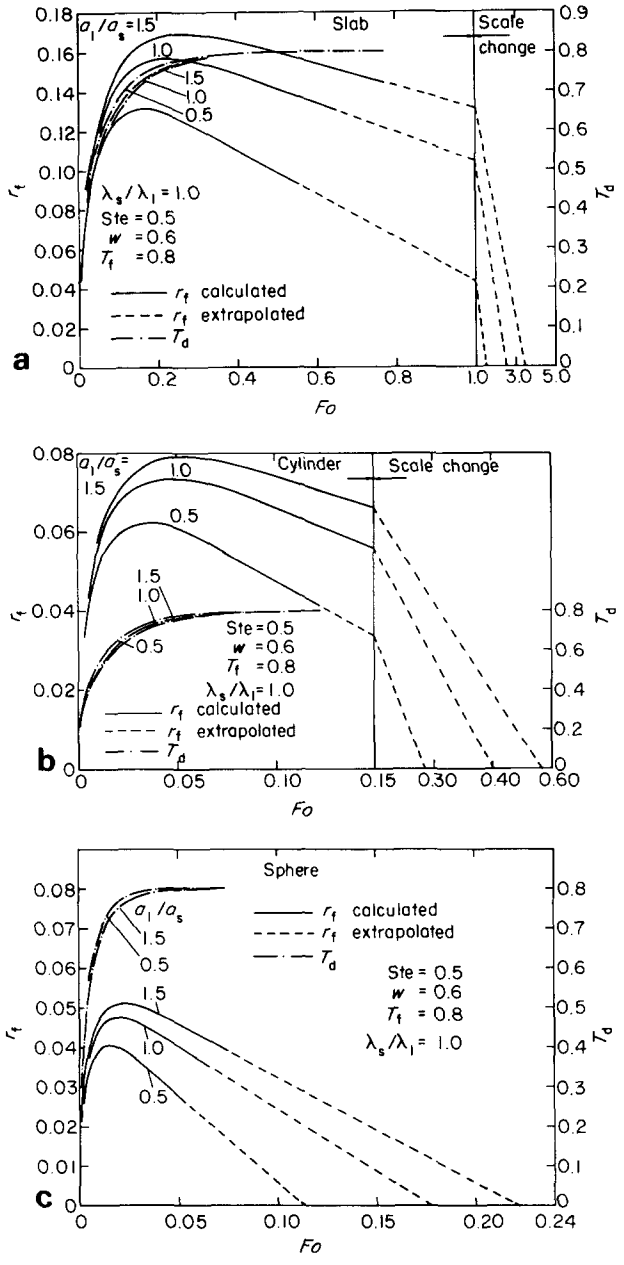

Fig 8 Effect of a_l/a_s *on* r_f *and* T_d *(a) slab insulated at one end (b) cylinder (c) sphere*

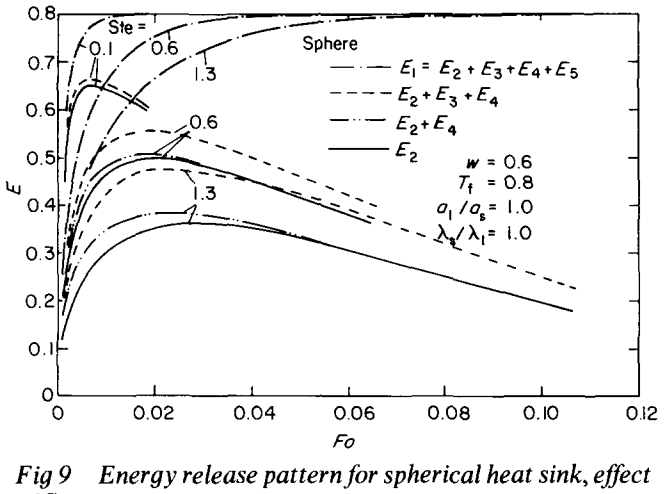

Fig 9 Energy release pattern for spherical heat sink, effect of Ste

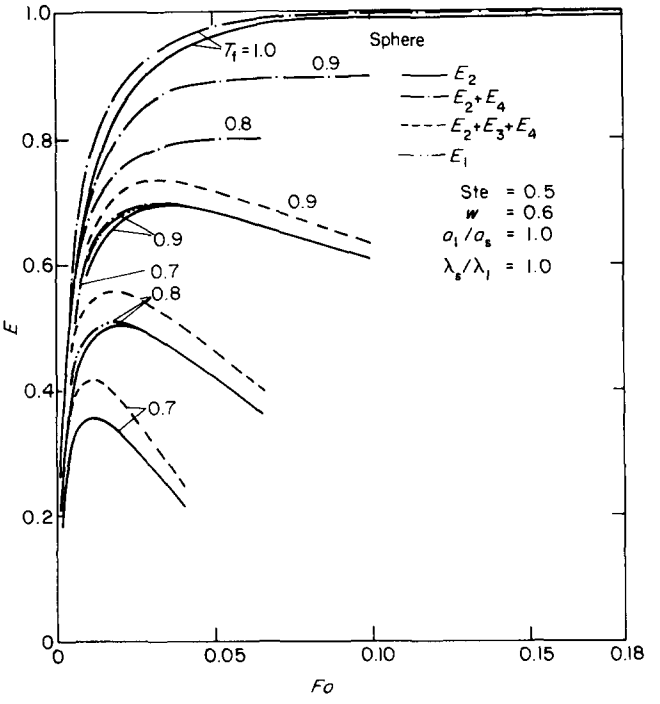

Fig 10 Energy release pattern for spherical heat sink, effect of T_f

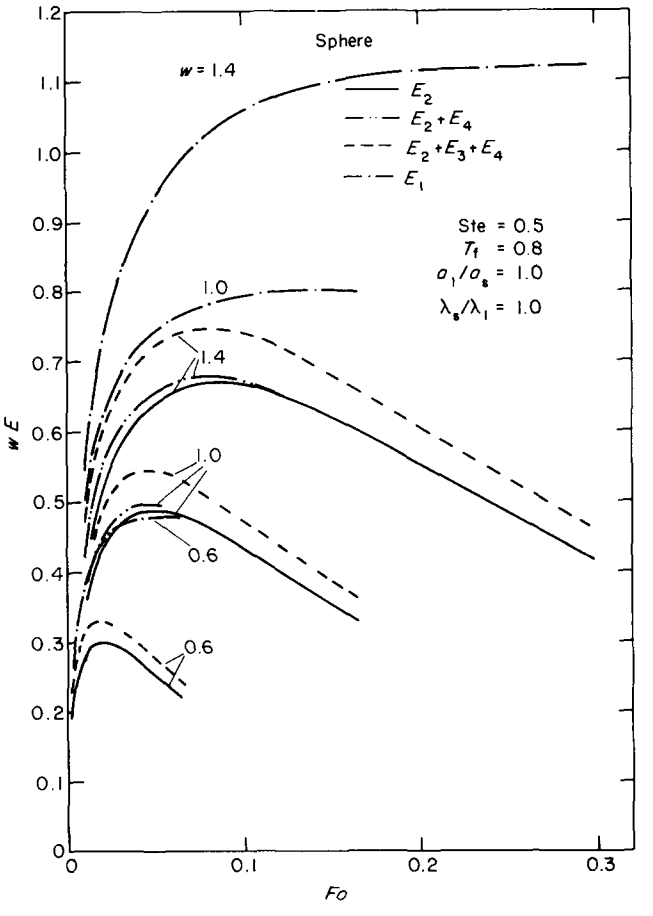

Fig 11 Energy release pattern for spherical heat sink, effect of w

both the phase change boundary and the drop absorb heat.

Since latent heat energy storage is of primary concern, the process should be stopped at time Fo^+, before the decay starts. Beyond this time, the sensible energy content is more and at Fo^{++}, it is totally a sensible heat storage device. Of the four components, the latent heat E_2 and the sensible heat E_5 are far greater than E_3 and E_4. In fact E_4 is so small that it cannot be separately plotted in Fig 8–10.

The influence of Stefan number on the energy components is seen in Fig 9. It may be observed that for smaller Stefan numbers:

- the latent heat energy released (E_2) is greater;
- the total energy extracted is higher;
- the latent heat component peak occurs at a smaller time, indicating a higher time rate of energy discharge.

Thus it is preferable to have low Stefan numbers which implies that either the pcm has a large latent heat, or that the initial temperatures of the two media are close to each other and not far from the freezing temperature, or both. But there are additional factors such as thermal cycling behaviour, suitability of freezing temperature to the particular application, corrosiveness, etc. to be considered. However, a Stefan number of 0.5 appears to be reasonable. For the combination of Hytherm 500 and nitrate eutectic, this gives a maximum temperature differential of 45.6 K with the freezing temperature being 495 K.

The liquid superheat T_f controls the energy components as shown in Fig 10. For larger values of T_f, the total energy extracted E_1, latent heat energy component E_2 and the peak values of E_1 and E_2 are higher. Such a behaviour is only to be expected, since lower T_f values mean more of sensible heat extraction. Therefore it is desirable to keep T_f as near to unity as possible. Since this is difficult to achieve, a value of $T_f = 0.8$ is taken as a realistic value.

The heat capacity ratio w plays a major role in the choice of the immiscible oil. Its effect on the energy components is shown in Fig 11. The enthalpy change of the heat transfer fluid drop, for a given temperature rise, is greater for fluids of larger heat capacities. So it is more appropriate to take the product of w and the energy components for a meaningful analysis. In Fig 11, the ordinate used is the product wE. Note that for large values of w the latent heat extracted and the total energy extracted are greater. Hence the choice should be a fluid of high volumetric specific heat. In practice, however, the selection is dictated by other factors like miscibility, flash point, viscosity, etc. The flash point of the fluid must be well above the pcm's freezing temperature and the viscosity must be low enough to avoid excessive carry over of pcm[4].

Since the latent heat component E_2 decreases beyond Fo^+, the heat transfer process must be stopped before then for lhtes devices. Fo^+ may be considered as the maximum residence time of the oil drops in a direct contact lhtes device.

Concluding remarks

Phase change around a heat sink involving the growth and subsequent decay of the freeze front and consequent changes in the sink temperature was analysed by finite difference methods. A parametric analysis of the heat transfer behaviour for a number sink geometries was carried out.

Energy components were estimated for the spherical heat sink applicable to direct contact lhtes devices. It is concluded that the following conditions are desirable:

(a) lower Stefan numbers;
(b) higher values of sink to pcm thermal capacity ratio, w;
(c) higher values of T_f (ie lower superheat);
(d) termination of the heat transfer process at time Fo^+.

References

1. **Tadjbakhsh J. and Liniger W.** Free boundary problems with regions of growth and decay – An analysis of heat transfer in dip soldering process. *Q.J. Mech. Appl. Math., 1964*, **17**(2), *141–155*
2. **Jiji L. M.** On the application of perturbation to free-boundary problems in radial systems. *J. Franklin Institute, 1970*, **289**(4), *281–291*
3. **Edie D. D. and Melsheimer S. S.** An immiscible fluid-heat of fusion energy system. *Proc. Int. Solar Energy Society, 1976*, **8**, *262–272*
4. **Edie D. D., Melsheimer S. S., Mullins J. J. and Mara J. F.** Latent heat storage using direct contact heat transfer. *Proc. Int. Solar Energy Society, 1979*, **1**, *640–644*
5. **Mills A. D., Melsheimer S. S. and Edie D. D.** Extended cycling behaviour of a direct contact-phase change TES problem. *AIChE Symposium Series, No. 198, Vol. 76, 1980, 41–46*
6. **Fouda A. E., Despault G. J. G., Taylor J. B. and Capes C. E.** Solar storage systems using salt hydrate latent heat and direct contact heat exchange – I Preliminary design considerations. *J. Solar Energy, 1980*, **25**, *437–444*
7. **Cease M. E.** A model of direct contact heat transfer for latent heat energy storage. *Proc. 15th IECE Conf. 1980*, **1**, *624–629*
8. **Helshoj E.** A high capacity, high speed latent heat storage unit. *Proc. ISES Congress, 1981*, **1**, *703–709*
9. **Solomon A. D.** Melt time and heat flux for a simple PCM body. *J. Solar Energy, 1979*, **22**, *251–257*
10. **Rose M. E.** A method for calculating solutions of parabolic equations with a free boundary. *Math. Comput., 1960*, **14**, *249–256*
11. **Bell G. E.** On the performance of the enthalpy method. *Int. J. Heat and Mass Transfer, 1982*, **25**(4), *587–589*
12. **Landau H. G.** Heat conduction in a melting solid. *Q. J. Appl. Math., 1950*, **8**(1), *81–94*
13. **von Rosenberg D. U.** Methods for the numerical solution of partial differential equations. *American Elsevier Publishing Co., New York, 1969, 113*
14. **Murray W. D. and Landis F.** Numerical and machine solutions of transient heat-conduction problems involving melting or freezing. *J. Heat Transfer, Trans. ASME, 1959*, **81**, *106–112*
15. **Kamimoto M., Tanaka T., Tani T. and Horigome T.** Investigation of nitrate salts for solar latent heat storage. *J. Solar Energy, 1980*, **24**, *581–587*
16. **Ferrara A., et al.** Thermal energy storage heat exchanger: molten salt heat exchanger design for utility power plants. *NASA Report No. CR 135244, 1977*
17. **Jurinak J. J. and Abdel-Khalik S. I.** On the performance of air based solar heating systems utilizing phase change energy storage. *Int. J. Energy, 1979*, **4**(4), *503–522*
18. HP Specialities – Technical information bulletin, *M/S Hindustan Petroleum Corporation, India*